

Supporting Information

Achieving Full-Color Emission of Cu Nanocluster Self-Assembly Nanosheets by virtue of Halogen Effects

Zhaoyu Liu,[†] Dong Yao,^{†,‡*} Lin Ai,^{†,§} Huiwen Liu,[†] Shitong Zhang,^{†,‡} and Hao Zhang^{†,§*}

[†]*State Key Laboratory of Supramolecular Structure and Materials, College of Chemistry, Jilin University, Changchun 130012, P. R. China, [‡]Institute of Theoretical Chemistry, Jilin University, Changchun 130023, P. R. China, and [§]Green Catalysis Center, College of Chemistry, Zhengzhou University, Zhengzhou, 450001, P. R. China.*

*Address correspondence to hao_zhang@jlu.edu.cn; dongyao@jlu.edu.cn.

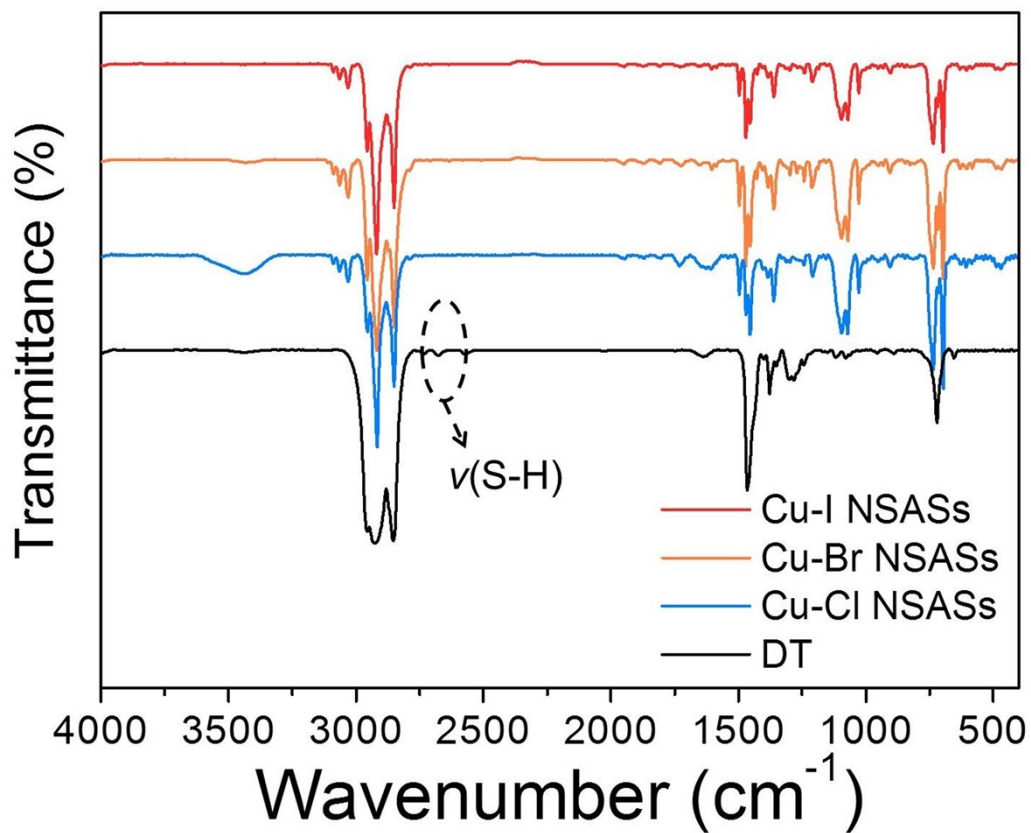


Fig. S1. FTIR spectra of pure DT and Cu-Cl, Cu-Br, and Cu-I NSASs. The disappearance of the S-H stretch peak at 2550 cm^{-1} in the Cu NSAS FTIR spectra indicates that DT is anchored to the Cu NSASs by forming Cu-S bonds.

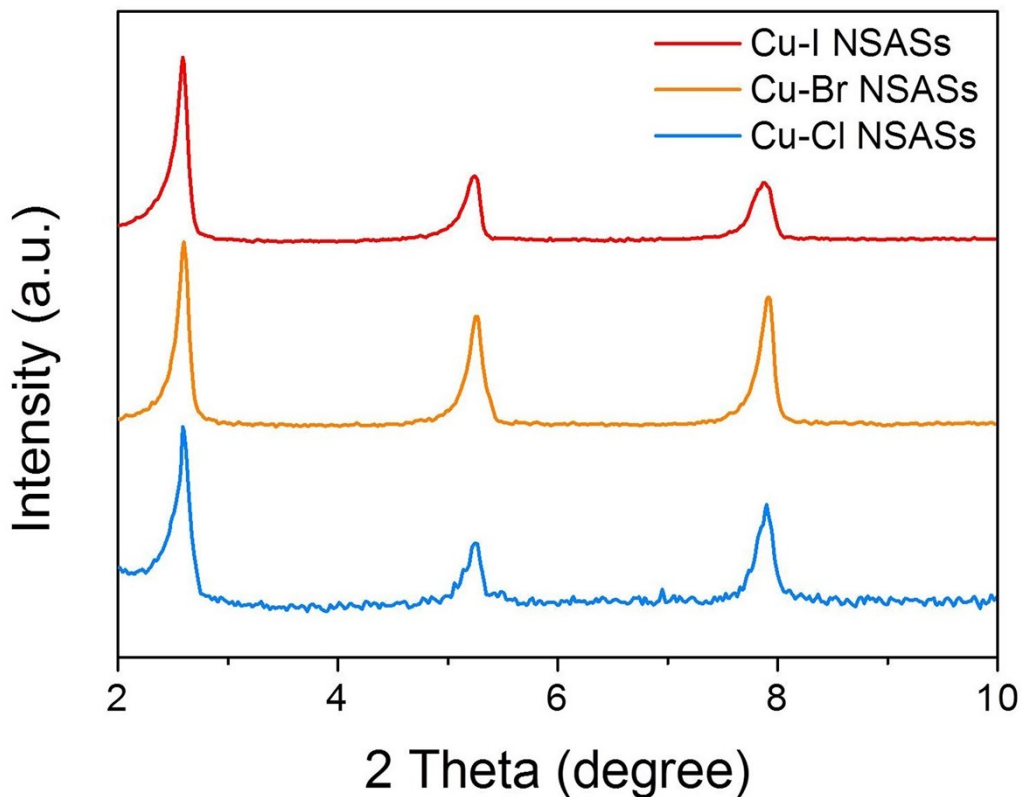


Fig. S2. Small-angle region of XRD patterns. Only one main diffraction peak appears at 2.6° and the second and third ordered peaks locate around 5.3 and 7.8° , which show that there is no difference in layer or cluster spacing between the three Cu NSASs.

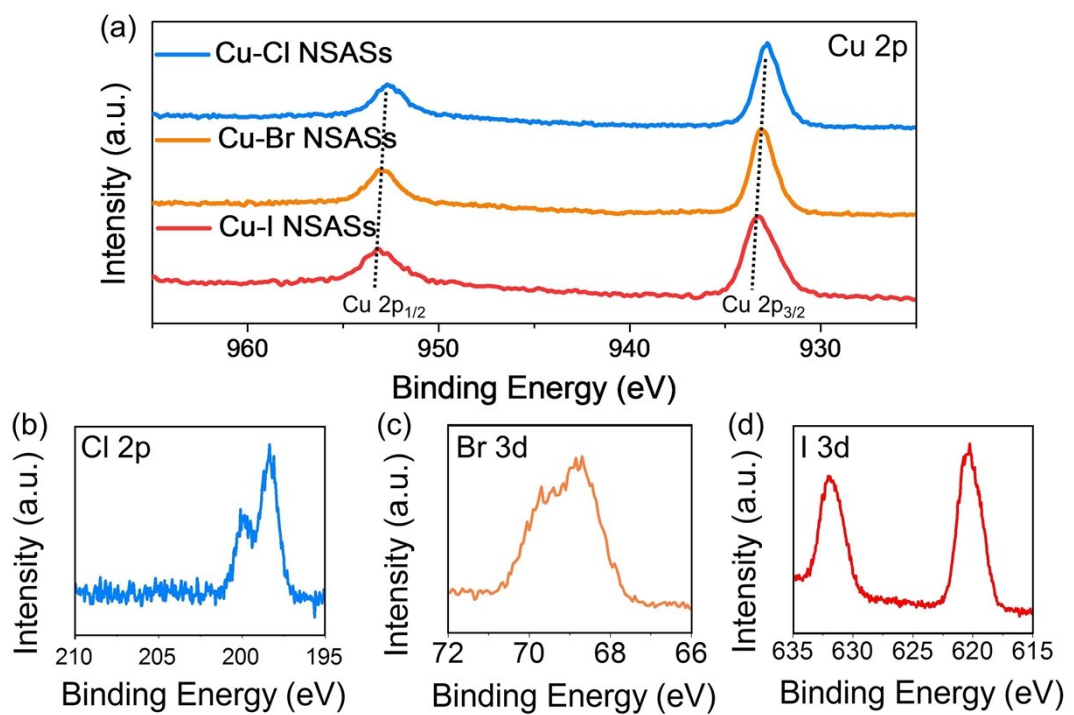


Fig. S3. (a) XPS Cu 2p spectra of the three Cu NSASs. XPS Cl 2p (b), Br 3d (c) and I 3d (d) spectra of Cu-Cl, Cu-Br and Cu-I NSASs.

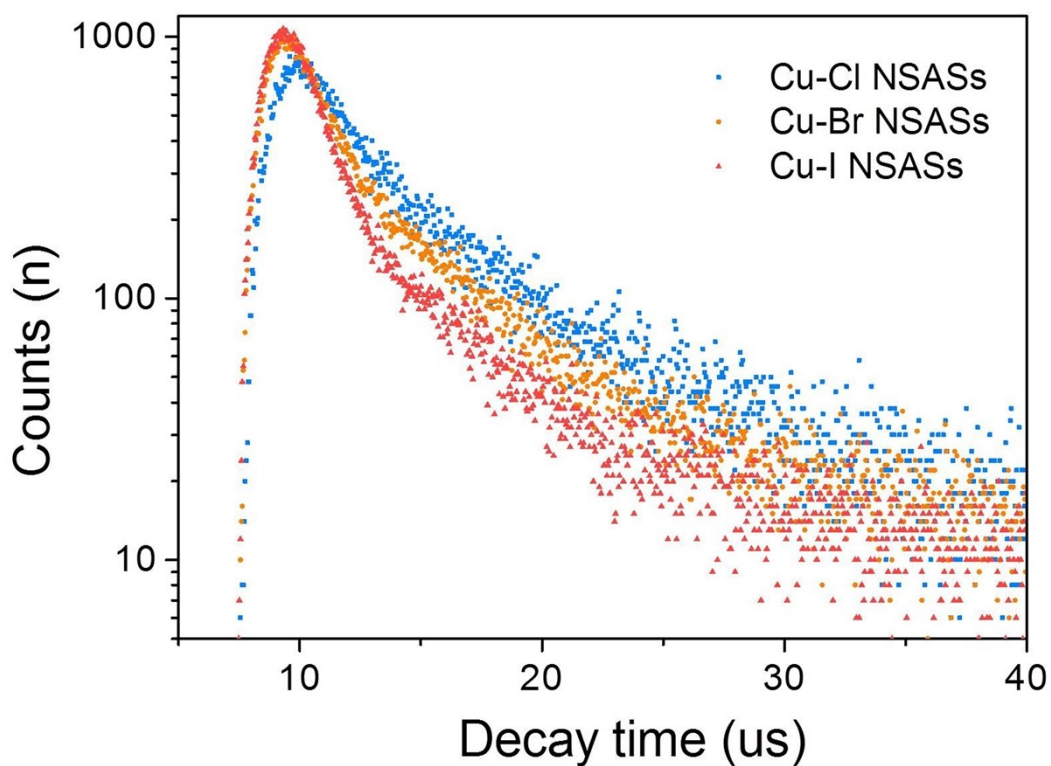


Fig. S4. PL decay curves of the Cu-Cl, Cu-Br and Cu-I NSASs detected at 365 nm.

Table S1. ^aEmission decay time, biexponential, ^bfast decay components and ^ccorresponding percentage, ^dslow decay components and ^ecorresponding percentage, and ^fphotoluminescent quantum yield of the Cu NSASs. ^gThe calculated rate of the intersystem crossing according to the equation $k_{ISC}=\Phi_{PL}\tau^l$, where Φ_{PL} represents photoluminescence quantum yield and τ represents emission decay time.

Cu NSASs	^a $\tau/\mu s$	^b $\tau_1/\mu s$	^c A ₁ (%)	^d $\tau_2/\mu s$	^e A ₂ (%)	^f $\Phi_{PL}(\%)$	^g $k_{ISC}/10^4 s^{-1}$
Cu-Cl	7.3	2.8	48.4	11.5	51.6	3.0	0.4
Cu-Br	4.4	1.9	49.3	6.8	50.7	4.4	1.0
Cu-I	3.5	1.4	58.9	6.4	41.1	8.0	2.3

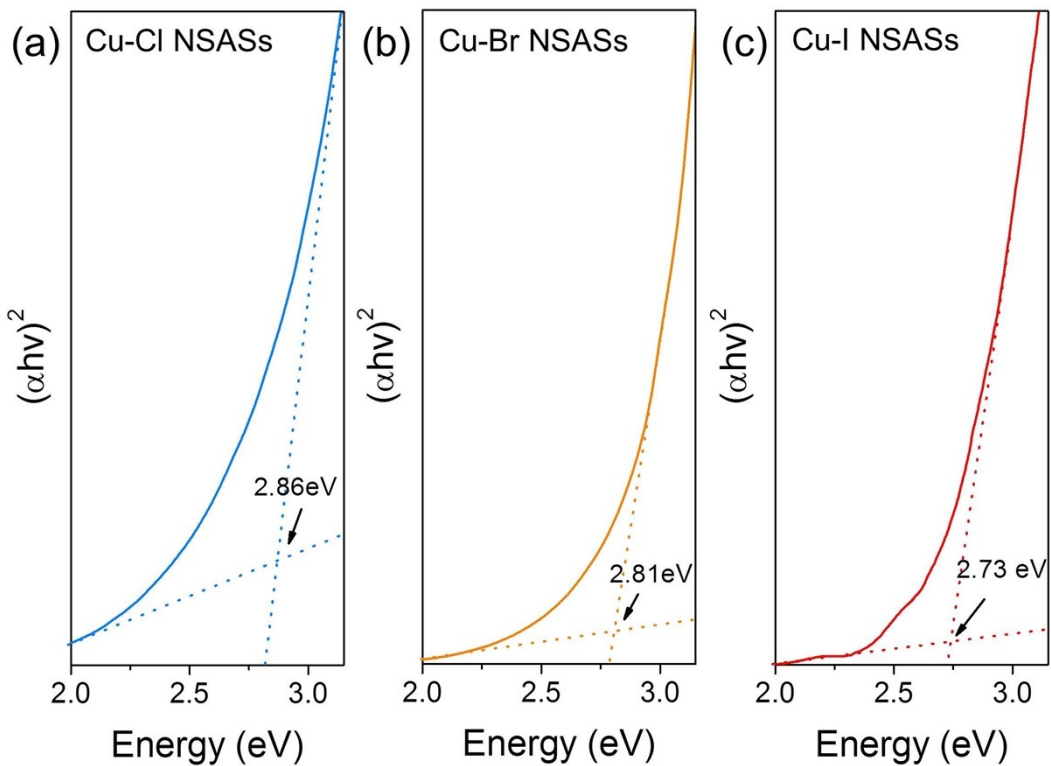


Fig. S5. The plot of $(\alpha h\nu)^2$ versus the photon energy of three Cu NSASs.

Table S2. Measured and Calculated Energy Gaps of Cu-Cl, Cu-Br and Cu-I NSASs.

^aDetermined from the plot of $(\alpha h\nu)^2$ versus the photon energy of three Cu NSASs based on

Fig. S3. ^bDetermined from the maximum of emission of the three Cu NSASs based on Fig. 3b.

^cCalculated from the difference between S₀T₁ gap and S₀S₁ gap.

Cu NSASs	^a S ₀ S ₁ gap (eV)	^b S ₀ T ₁ gap (eV)	^c S ₁ T ₁ gap (eV)
Cu-Cl	2.9	2.5	0.4
Cu-Br	2.8	2.2	0.6
Cu-I	2.7	1.8	0.9

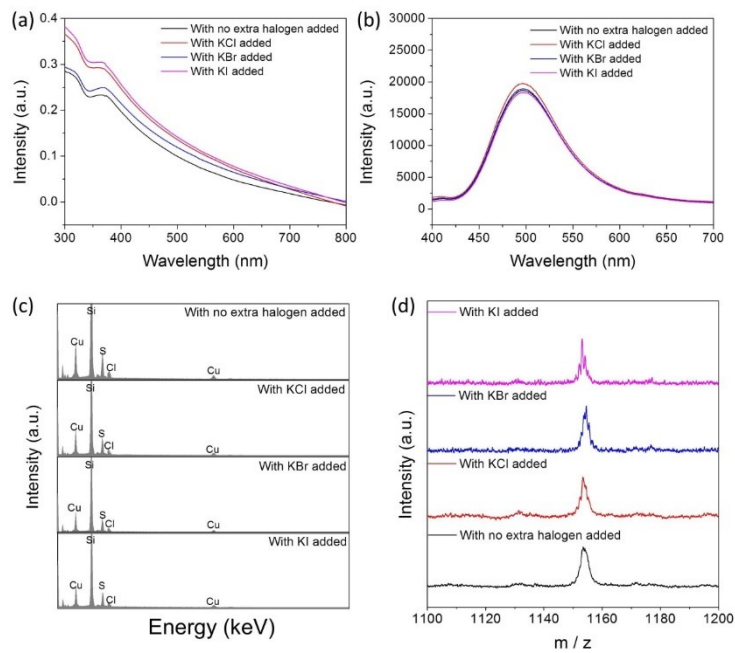
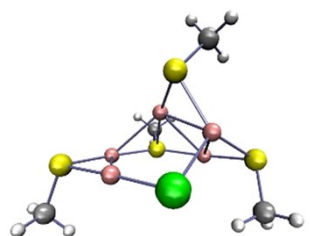
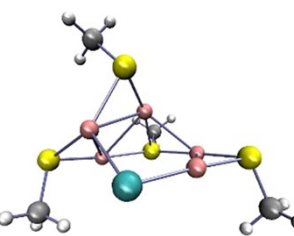


Fig. S6. (a) UV-vis absorption spectra, (b) PL emission spectra, (c) EDS spectra and (d) MALDI-TOF mass spectra of the Cu-Cl NSASs with and without the addition potassium halides.

Cu-Cl NC



Cu-Br NC



Cu-I NC

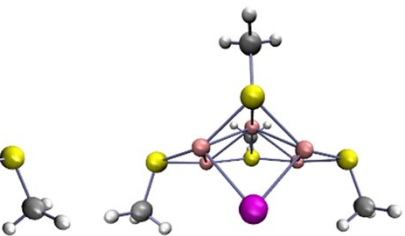


Fig. S7. Simulated structure of the Cu-Cl, Cu-Br and Cu-I NCs. Simplistically, CH₃SH is selected as the capping ligand instead of DT. Color labels: Pink, Cu; silver, C; white, H; yellow, S; green, Cl; cyan, Br; magenta I; red, wave function positive phase and blue, wave function negative phase.

Table S3. The atomic positions (in Å) of DFT-optimized Cu-Cl NC.

Atom	X	Y	Z
Cu1	-2.13466	1.04613	-0.21373
Cu2	-1.73073	-1.6403	0.053664
Cu3	1.713739	-1.09464	0.41993
Cu4	1.569378	1.071298	-1.21882
Cu5	0.232778	1.022184	1.028185
S6	1.055535	-0.38023	2.537379
C7	2.511281	0.531552	3.247883
H8	2.166344	1.213382	4.022977
H9	3.179241	-0.20412	3.692173
H10	3.051599	1.084322	2.483973
S11	-3.60354	-0.48432	0.398286
C12	-4.65351	-0.83058	-1.09901
H13	-5.4247	-0.06578	-1.1609
H14	-4.06594	-0.83494	-2.01219
H15	-5.12011	-1.80367	-0.96277
S16	-0.34616	2.237834	-0.83646
C17	-0.28001	4.037596	-0.38825
H18	-0.56174	4.61165	-1.26758
H19	-0.97339	4.231986	0.424484
H20	0.731079	4.292224	-0.08446
S21	3.187761	-0.43185	-1.23858
C22	2.860179	-1.53002	-2.6998
H23	3.077522	-0.9874	-3.61742
H24	3.530052	-2.38435	-2.62053
H25	1.832783	-1.88299	-2.70029
Cl26	0.081612	-2.78353	-0.37295

Table S4. The atomic positions (in Å) of DFT-optimized Cu-Br NC.

Atom	X	Y	Z
Cu1	-1.57583	1.224909	-1.23482
Cu2	-1.74548	-0.86647	0.498885
Cu3	1.778667	-1.4672	0.153093
Cu4	2.160838	1.206805	-0.2726
Cu5	-0.19048	1.236778	0.980285
S6	-1.04073	-0.05532	2.569533
C7	-2.45345	0.945625	3.245462
H8	-2.98868	1.469768	2.458089
H9	-3.13735	0.260424	3.743028
H10	-2.07403	1.66056	3.973245
S11	-3.24514	-0.2186	-1.14546
C12	-3.01344	-1.37625	-2.57811
H13	-3.26632	-0.86239	-3.50314
H14	-1.99439	-1.75061	-2.6187
H15	-3.69464	-2.21295	-2.4342
S16	0.370797	2.36807	-0.94601
C17	0.316818	4.182866	-0.55953
H18	0.562805	4.724791	-1.46945
H19	-0.6818	4.448382	-0.22557
H20	1.041485	4.40722	0.217352
S21	3.645288	-0.27157	0.420678
C22	4.690277	-0.69672	-1.05972
H23	5.450934	0.072374	-1.17487
H24	5.170432	-1.65338	-0.86631
H25	4.096904	-0.76584	-1.96652
Br26	-0.10897	-2.74293	-0.24063

Table S5. The atomic positions (in Å) of DFT-optimized Cu-I NC.

Atom	X	Y	Z
Cu1	-1.92625	1.507577	-0.72577
Cu2	-1.76095	-0.84313	0.673004
Cu3	1.699385	-0.95593	0.600562
Cu4	2.027487	1.434711	-0.68278
Cu5	0.028025	1.110122	0.920415
S6	-0.03729	-0.63998	2.308315
C7	-0.08393	0.140183	3.982072
H8	-0.95316	0.786681	4.073563
H9	-0.15072	-0.6626	4.714031
H10	0.825502	0.711049	4.153643
S11	-3.6058	0.184938	-0.19815
C12	-4.02434	-0.7574	-1.72389
H13	-4.56291	-0.10638	-2.40961
H14	-3.1323	-1.15076	-2.20355
H15	-4.66953	-1.58458	-1.43344
S16	0.074605	2.546175	-0.87816
C17	0.099603	4.293553	-0.30336
H18	0.113491	4.932629	-1.18334
H19	-0.78902	4.497842	0.286643
H20	0.989413	4.469342	0.29398
S21	3.629799	0.036474	-0.11376
C22	4.101785	-0.86969	-1.64688
H23	4.702481	-0.21709	-2.27722
H24	4.698694	-1.73003	-1.34975
H25	3.226166	-1.21239	-2.19106
I26	-0.07172	-2.35778	-0.81115

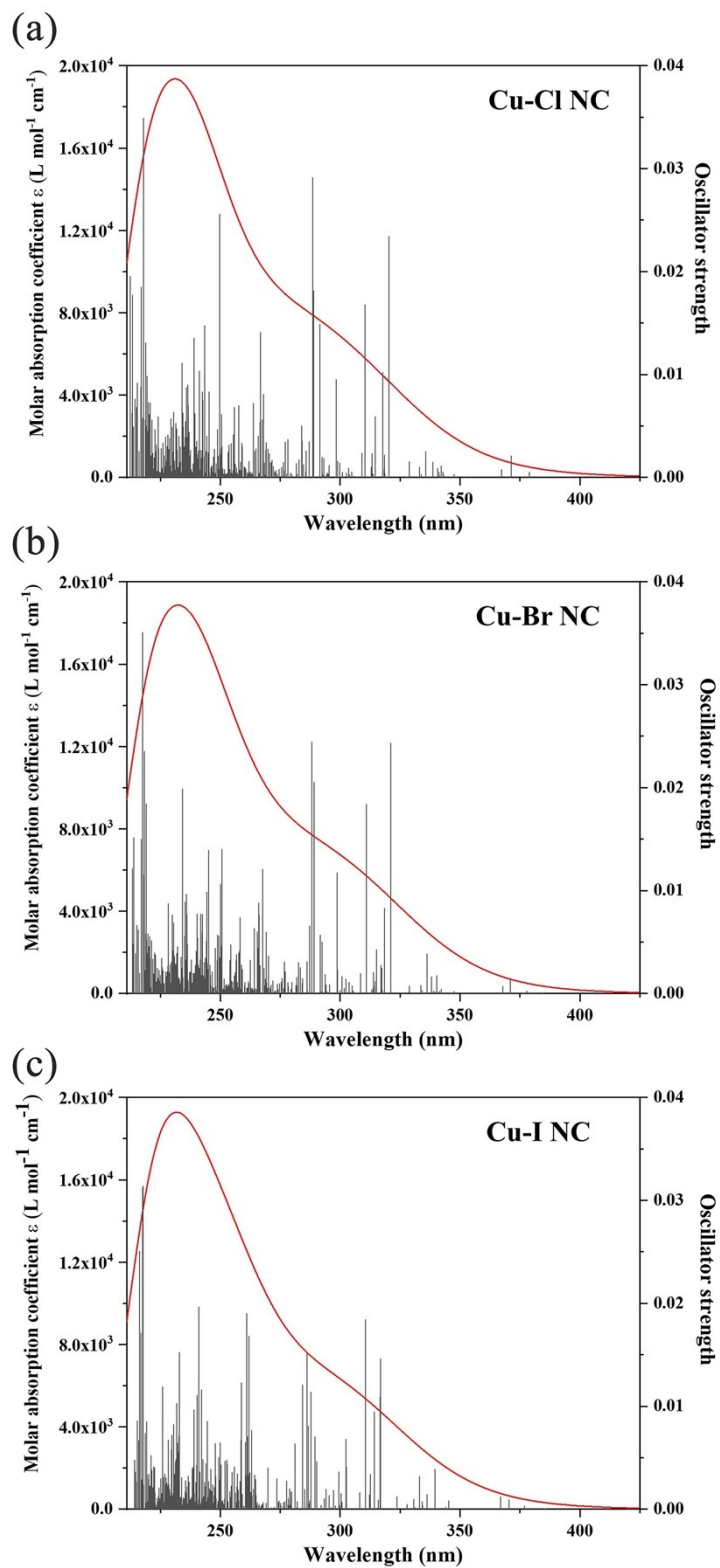


Fig. S8. Spin-orbit coupling (SOC) corrected UV-vis spectrum of the Cu-Cl (a), Cu-Br (b) and Cu-I (c) NCs. Red line: Fitted curves made by molar absorption coefficient; Black line: Excitation energy and corresponding oscillator strength.

Table S6. DFT calculated ^aS₀T₁ gap, ^bSOC between S₀ and T₁ state and ^cSOC between S₁ and T₁ of the Cu-Cl, Cu-Br and Cu-I NCs.

Cu NC	^a S ₀ T ₁ gap/eV	^b <S ₀ SOC T ₁ >/cm ⁻¹	^c <S ₁ SOC T ₁ >/cm ⁻¹
Cu-Cl	2.52	33.10	28.04
Cu-Br	1.08	50.39	29.34
Cu-I	0.76	54.00	30.78

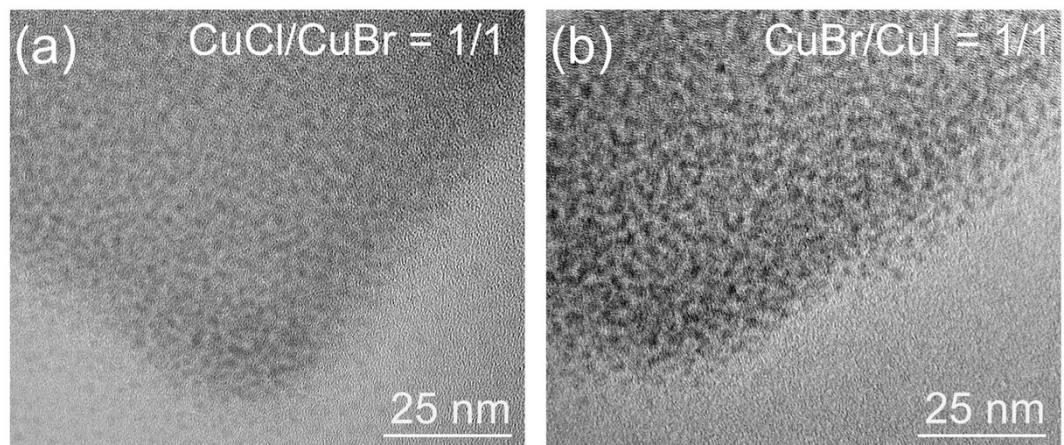


Fig. S9. TEM images of the Cu NCASSs obtained with mixed Cu sources. (a) CuCl and CuBr and (b) CuBr and CuI with equimolar ratios.

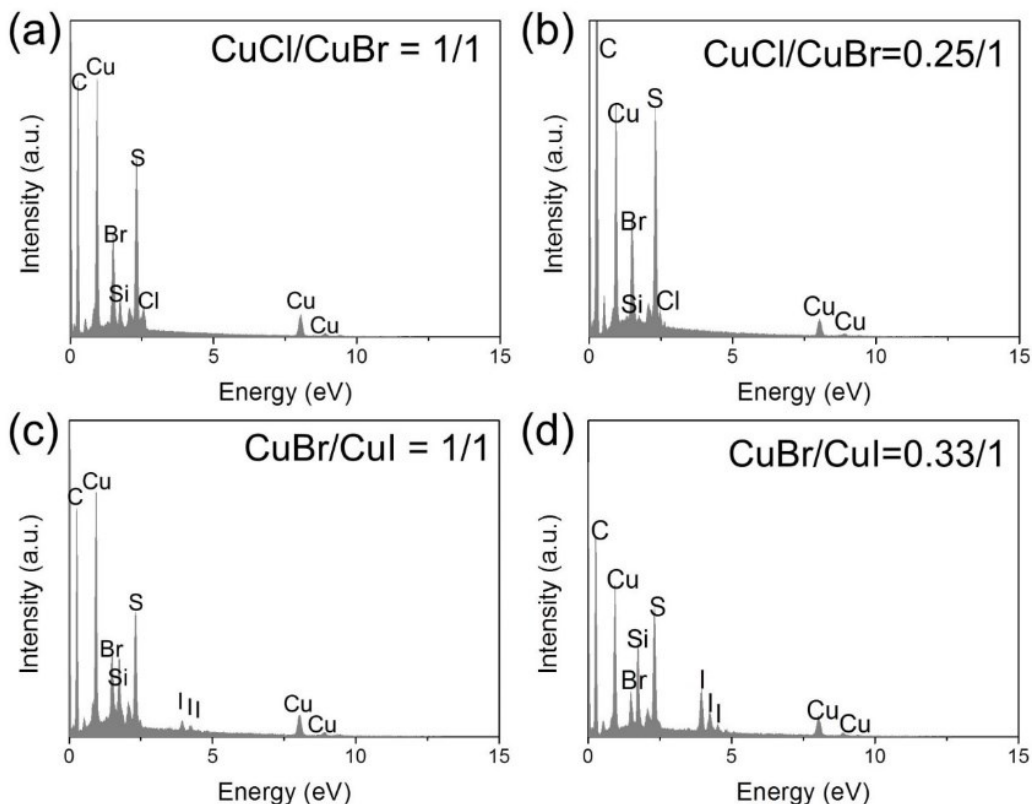


Fig. S10. EDS analysis of the composition of the Cu NCASs obtained with mixed Cu sources with different feed molar ratio: (a) CuCl/CuBr=1/1, (b) CuCl/CuBr=0.25/1, (c) CuBr /CuI=1/1, and (d) CuBr /CuI=0.33/1. The Cu/S/Cl/Br molar ratio is 8.3/6.8/0.7/1.0 in (a) and 24.6/19.8/1.0/4.1 in (b). The Cu/S/Br/I molar ratio is 11.5/9.2/1.3/1.0 in (c) and 19.9/14.7/1.0/2.9 in (d). Note that the signals of Si are resulted from the substrate.

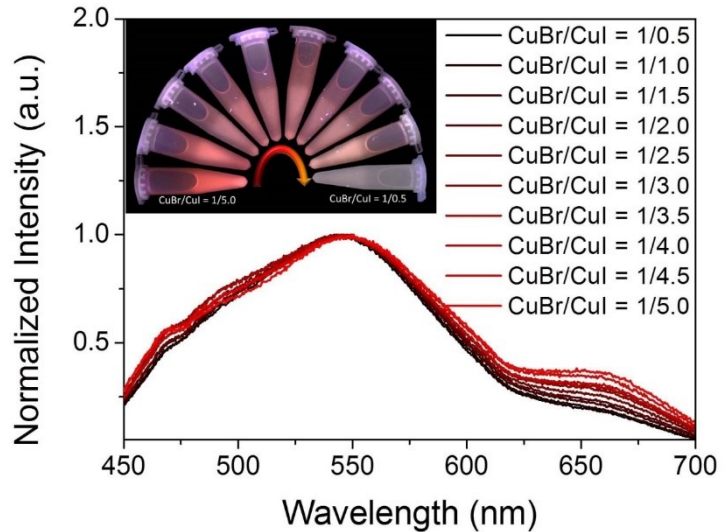


Fig. S11. PL emission spectra of the Cu NCASs obtained with different feed molar ratio of CuBr and CuI as the Cu source. Inset is the corresponding PL emission image under 365 nm excitation.

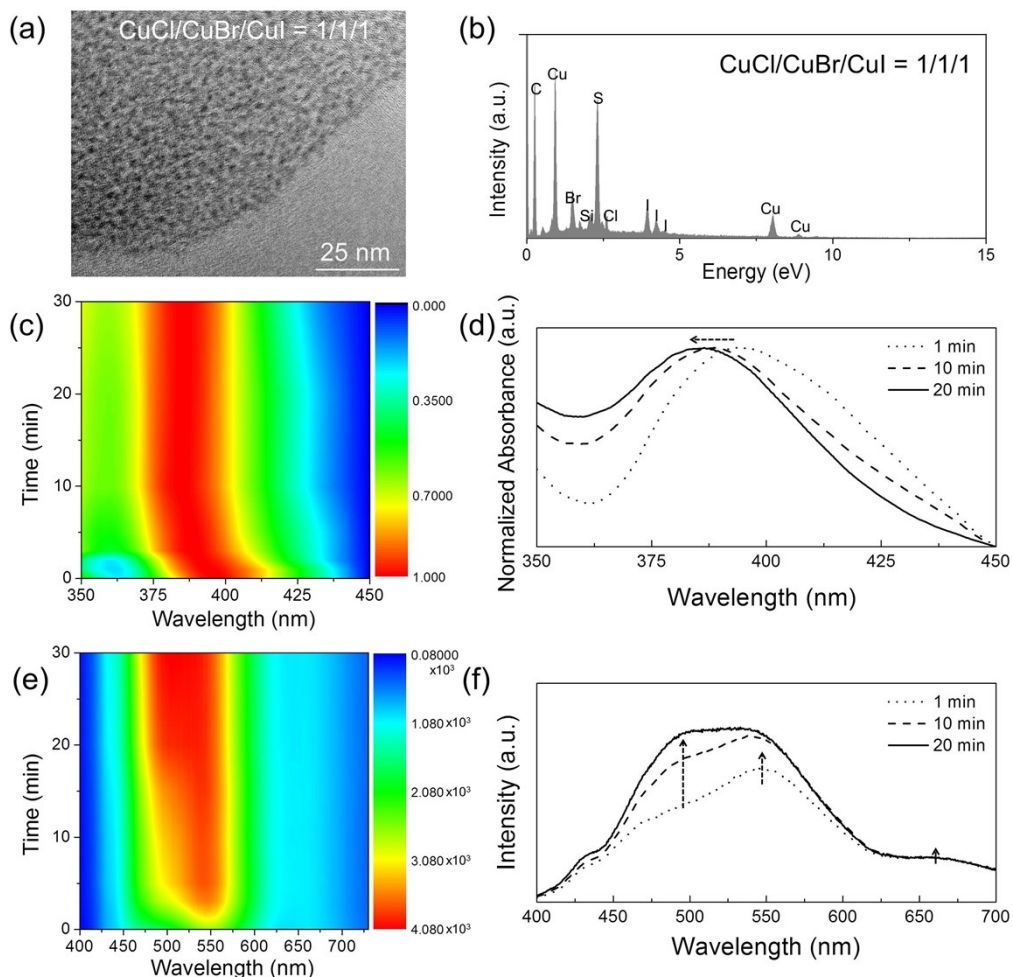


Fig. S12. (a) TEM images of the Cu NCASs obtained with equimolar amount of CuCl, CuBr and CuI as the Cu sources. (b) EDS analysis of the composition of the obtained Cu NCASs. The Cu/S/Cl/Br/I molar ratio is 15.3/13.1/0.8/1.3/1.0. (c) Time-dependent normalized absorption contour of the formation of the Cu NCASs and (d) the corresponding spectrum at 1, 10 and 20 min. (e) Time-dependent PL intensity contour of the Cu NCASs and (f) the corresponding spectrum at 1, 10 and 20 min.

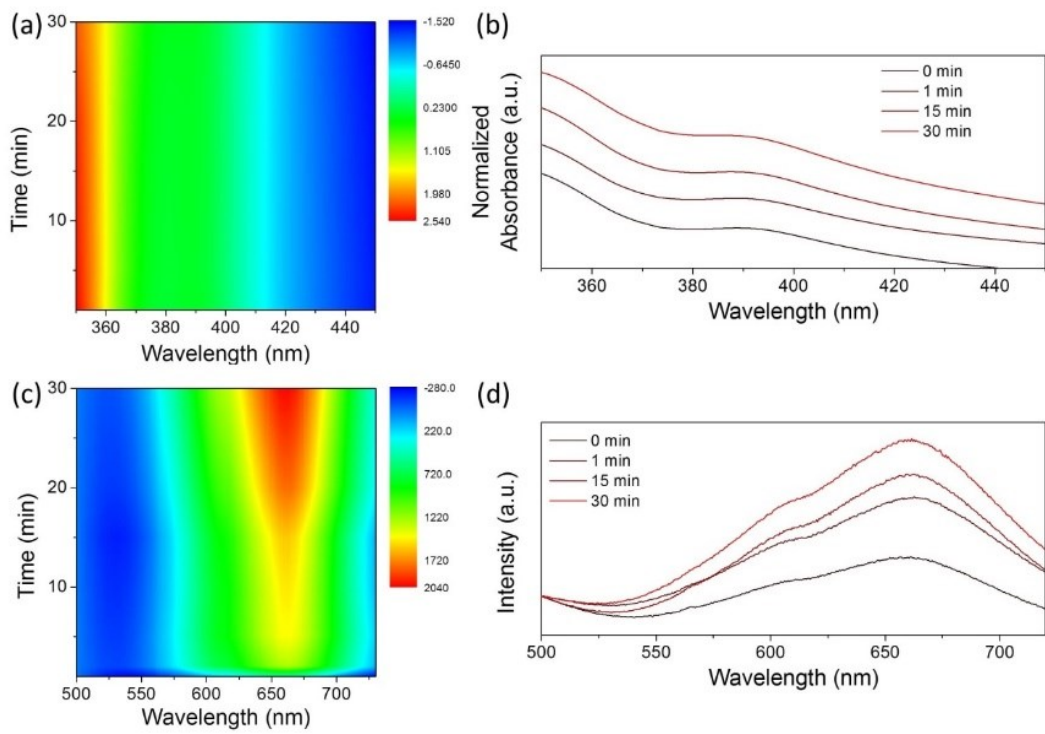


Fig. S13. (a) Time-dependent normalized absorption contour of the formation of the Cu-I NSAS and (b) the corresponding spectra at specific time. (c) Time-dependent PL intensity contour of the Cu-I NSAS and (d) the corresponding spectra at specific time.

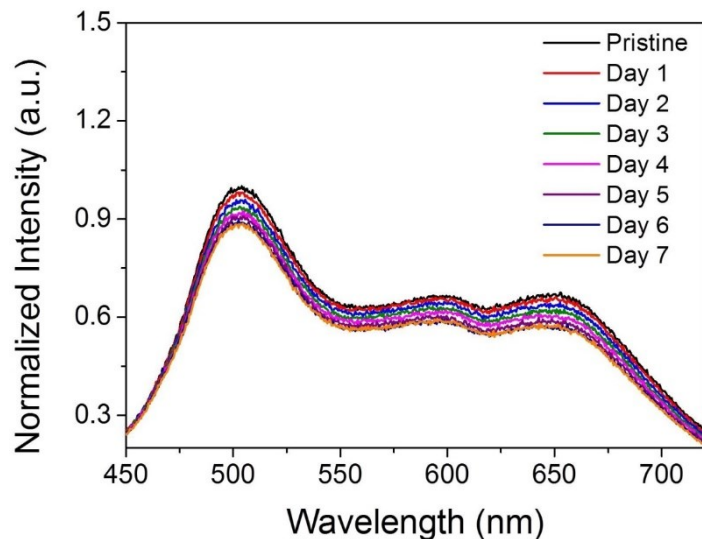


Fig. S14. The PL emission spectra of the Cu NCAs obtained with equimolar amount of CuCl, CuBr and CuI as the Cu source at different storage time.

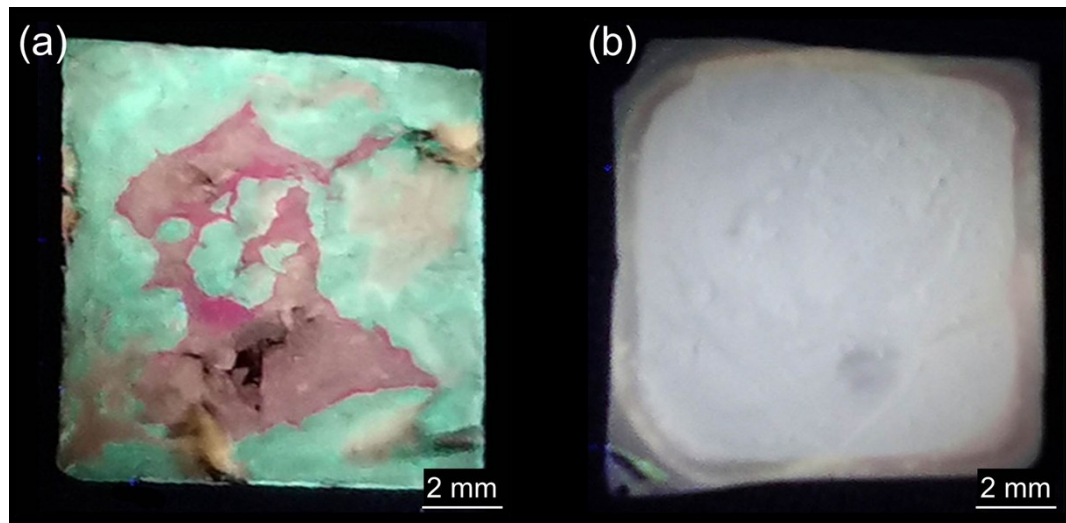


Fig. S15. Photographs of silicon slices under 365 nm excitation with different solution deposited. (a) Mixture comprised of equimolar amount of Cu-Cl, Cu-Br and Cu-I NSAs and (b) Cu NCAs obtained with equimolar amount of CuCl, CuBr and CuI as the copper source.

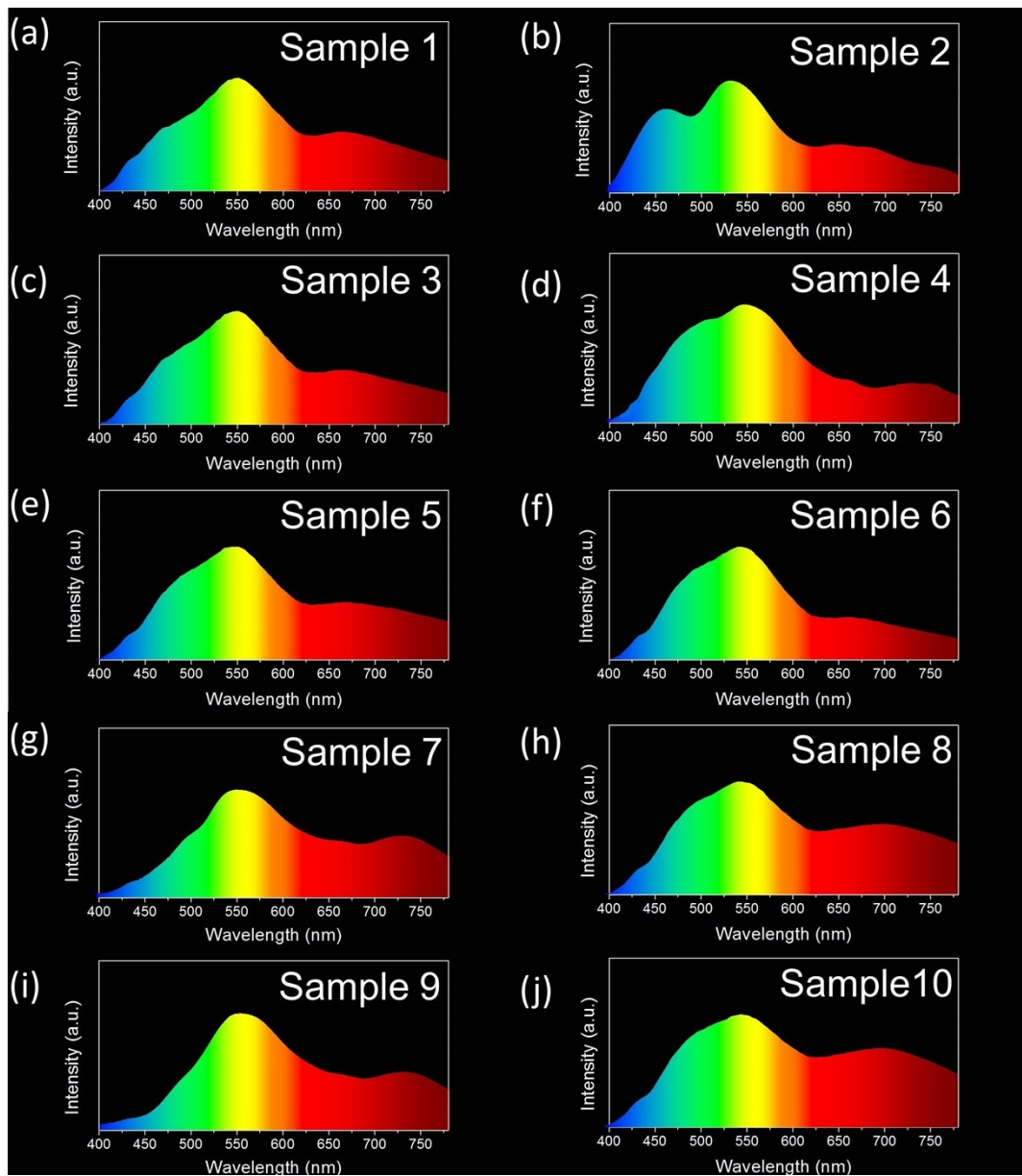


Fig. S16. Emission spectra of WLEDs based on Cu NCASs with different Cl/Br/I feed molar ratios.

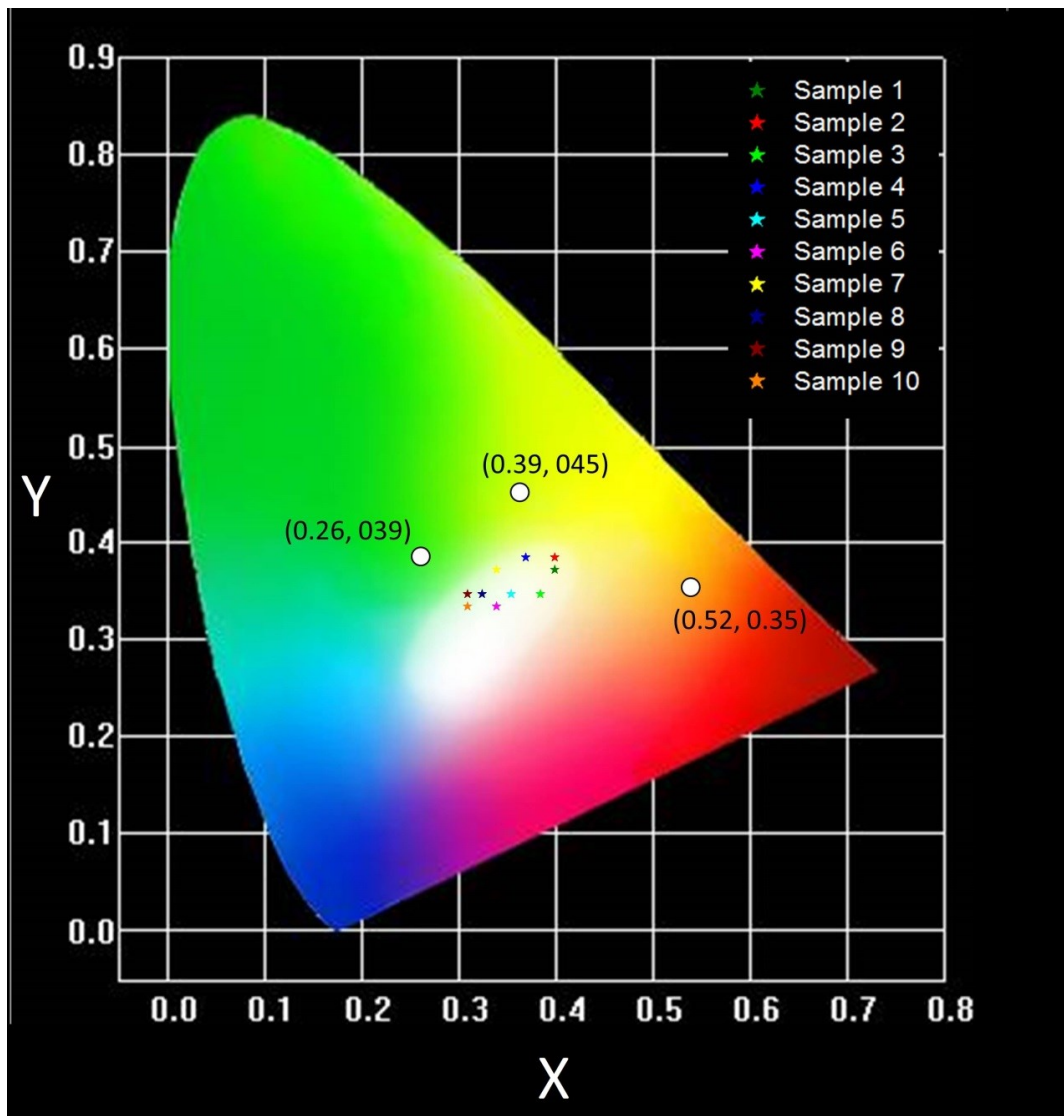


Fig. S17. The CIE chromaticity coordinates of the LEDs based on the Cu NSAs and NCAsSs.

Fig. 6e is a partial enlarged view of the Fig. S17.

Table S7. Color coordinates and color temperatures of the WLEDs based on the Cu NCAs with different Cl/Br/I feed molar ratios.

Sample	Cl/Br/I feed molar ratio	Color coordinate	Color temperature/K	CRI
1	0.8/1.0/2.1	(0.37, 0.38)	4313	88
2	0.8/1.0/1.9	(0.37, 0.39)	4365	92
3	0.8/1.0/1.7	(0.36, 0.36)	4387	87
4	0.8/1.0/1.5	(0.35, 0.39)	4881	83
5	0.8/1.0/1.3	(0.34, 0.36)	5186	91
6	1.1/1.0/1.3	(0.33, 0.35)	5574	80
7	1.25/1.0/1.3	(0.33, 0.38)	5706	78
8	1.4/1.0/1.3	(0.32, 0.36)	6041	80
9	1.55/1.0/1.3	(0.31, 0.36)	6323	81
10	1.7/1.0/1.3	(0.31, 0.35)	6559	85